7.12: Rubredoxin- A Single-Fe Tetrathiolate Protein

The physiological role of rubredoxins (sometimes abbreviated as Rd) is not always known with certainty. In particular, although rubredoxin was first identified[26] in the anaerobe *Clostridium pasteurianum*, its role in anaerobic metabolism remains obscure. Some rubredoxins, such as that from the aerobe *Pseudomonas oleovorans*, participate in fatty acid ω-hydroxylation, i.e., hydroxylation at the end of the hydrocarbon chain farthest from the carboxylic acid.[27] Like the Fe_2S_2 proteins putidaredoxin[28] and adrenodoxin,[29] the rubredoxin provides electrons to the hydroxylase, which acts as a monooxygenase forming the w-alcohol product and water (see Figure 7.3). In a reaction catalyzed by rubredoxin reductase, rubredoxin is reduced by NADH to the ferrous state and reoxidized by the w-hydroxylase to the ferric form during the catalytic cycle.

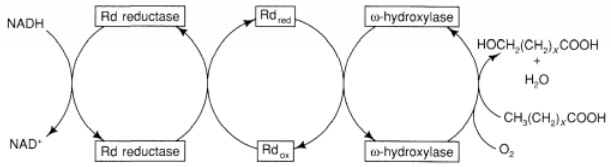

Figure 7.3 - Diagram illustrating the redox changes that occur in the rubredoxin-dependent ω-hydroxylase of Pseudomonas oleovorans.[27]

Most rubredoxins contain a single Fe atom, which can exist in the ferrous or ferric state. For the rubredoxin from Clostridium pasteurianum,[26] the E°' value is -57 mV, which is much more positive than that of ferredoxins from the same organism (see below). The 6-kDa clostridial protein has only 54 amino acids in its polypeptide chain, and has a very low isoelectric point of 2.93. The rubredoxin from *P. oleovorans*[27] has one or two iron atoms in a single polypeptide chain of MW ~ 20 kDa. Its redox potential is -37 mV for the $Fe^{3+/2+}$ couple. Rubredoxins as a class show considerable sequence identity, and the larger 2Fe members of the class show evidence, involving internal-sequence homology, that they may have. evolved through gene duplication.

A protein from *Desulfovibrio gigas*, called desulforedoxin,[30,31] appears to resemble rubredoxins in some respects, but the two Fe atoms in the 7.6-kDa protein appear to be spectroscopically and structurally distinct from the Fe atoms in rubredoxins.[31] A protein from *Desulfovibrio vulgaris* called ruberythrin has a single rubredoxin site as well as a strongly coupled 2Fe site resembling that of hemerythrin. Its physiological function is unknown. Table 7.1 lists some of the known rubredoxins and their properties.

Table 7.1 - Properties of some iron-sulfur proteins.

a) g'-tensors for $\pm \frac{1}{2}$ and $\pm \frac{3}{2}$ Kramers doublets, respectively, of the S = $\frac{5}{2}$ system. The values of 0.9 and 1.25 are calculated (not observed)[44]

b) The fully reduced protein has a complex spectrum due to magnetic coupling between the two identical Fe_4S_4 clusters. The g-values are those for partly reduced samples, and represent a magnetically isolated cluster.

c) The reported spectrum is complex because of magnetic interaction with the reduced Fe_3S_4 cluster.

d) Recent evidence suggests that *Thermus thermophilus* and *Thermus aquaticus* are actually the same species.[362] EPR parameters of the homologous *Thermus thermophilus* ferredoxin estimated from computer simulations.[361] In this protein a signal originating from the Fe_3S_4 cluster at g' $\simeq$ 12, attributable to $\Delta M_s = \pm 4$ transitions, is observed for the reduced (S = 2) cluster.

Protein Source	Molecular Weight (subunits)	Fe-S Composition	Redox Potention mV (pH)	EPR g values			References
Rubredoxins							
Clostridium pasteurianum	6,000	Fe	-58 (7)	9.3	4.3		26
Pseudomonas oleovorans	6,000	Fe		9.42 4.02	0.9 4.77	1.25[a] 4.31	44

Protein Source	Molecular Weight (subunits)	Fe-S Composition	Redox Potention mV (pH)	EPR g values			References
Fe_2S_2 Proteins							
Spinach ferredoxin	11,000	[2Fe-2S]	-420 (7.0)	2.05	1.96	1.89	350, 351
Parsley ferredoxin	11,000	[2Fe-2S]		2.05	1.96	1.90	352
Euglena ferredoxin	11,000	[2Fe-2S]		2.06	1.96	1.89	352
Adrenal cortex ferredoxin (pig) [Adrenodoxin]	16,000	[2Fe-2S]	-270 (7.0)	2.02	1.93	1.93	352, 353
Pseudomonas putida ferredoxin [Putidaredoxin]	12,500	[2Fe-2S]	-240 (7.0)	2.02	1.93	1.93	352, 353
Clostridium pasteurianum	25,000	[2Fe-2S]	-300 (7.5)	2.00	1.96	1.94	354
Xanthine Oxidase	280,000 (2)	2 x [2Fe-2S] I II	-343 (8.2) -303 (8.2)	2.02 2.12	1.94 2.01	1.90 1.91	355, 356
Thermus thermophilus Rieske	20,000	2 x [2Fe-2S]	+150 (7.8)	2.02	1.90	1.80	93, 357
Fe_4S_4 Proteins							
Clostridium pasteurianum	6,000	2 x [4Fe-4S]	-420 (8.2)	2.06	1.92	1.89[b]	115
Bacillus stearothermophilus	9,100	[4Fe-4S]	-280 (8.0)	2.06	1.92	1.89	358
Desulfovibrio gigas ferredoxin I	18,000 (3)	[4Fe-4S]	-455 (8.0)	2.07	1.94	1.92	359
Aconitase (beef heart) [active]	81,000	[4Fe-4S]		2.06	1.93	1.86	
Chromatium vinosum HiPIP	10,000	[4Fe-4S]	+356 (7.0)	2.12	2.04	2.04	353

Protein Source	Molecular Weight (subunits)	Fe-S Composition	Redox Potention mV (pH)	EPR g values			References
Paracoccus sp.	10,000	[4Fe-4S]	+282 (7.0)				353
Azotobacter vinlandii Fd I	14,500	[3Fe-4S] [4Fe-4S]	-645 (8.3)	2.06	1.93	1.89[c]	360
Thermus aquaticus	10,500	[3Fe-4S] [4Fe-4S]	-550 (9.0)	2.06	1.93	1.92[c]	353, 361
Fe_3S_4 Proteins							
Desulfovibrio gigas Fd II	6,000 (4)	[3Fe-4S]	-130 (8.0)	2.02			359
Azotobacter vinlandii Fd I	14,500	[3Fe-4S] [4Fe-4S]	-450 (8.3)	2.01			360
Thermus aquaticus	10,500	[3Fe-4S] [4Fe-4S]	-260 (9.0)	2.02	1.99	1.94[d]	353, 361
Aconitase (beef heart) [inactive]	81,000	[3Fe-4S]		2.01			

The x-ray crystal structures of the rubredoxins from *C. pasteurianum*[32] and *D. vulgaris*[33] have been determined.[33a] The *C. pasteurianum* protein structure is known to a resolution of 1.2 Å, placing it among the metalloproteins whose structures are known with greatest precision. The individual Fe and S atoms are clearly resolvable. As shown in Figure 7.4, the single iron is coordinated by four S ligands provided by Cys-6, Cys-9, Cys-39, and Cys-42. The sequence Cys-x-y-Cys is a common one in Fe-S proteins, because it allows both cysteine residues to bind to the same metal site or cluster. The Fe-S distances and angles in the clostridial rubredoxin are shown in Table 7.2. The range of distances and angles reveals a slightly distorted tetrahedral structure.

Figure 7.4 - The x-ray crystal structure of rubredoxin from Clostridium pasteurianum.[32]

Table 7.2 - Bond distances and bond angles around Fe in rubredoxin from *Clostridium pasteurianum* (W1).[32]

	Distance (Å)
Fe-S[Cys(6)]	2.33(11)
Fe-S[Cys(9)]	2.288(15)
Fe-S[Cys(39)]	2.300(15)
Fe-S[Cys(42)]	2.235(12)

	Angle (°)
S-Fe-S[Cys(6)-Fe-Cys(9)]	113.8 (4)
S-Fe-S[Cys(6)-Fe-Cys(39)]	109.0 (4)
S-Fe-S[Cys(6)-Fe-Cys(42)]	103.8 (4)
S-Fe-S[Cys(9)-Fe-Cys(39)]	103.7 (4)
S-Fe-S[Cys(9)-Fe-Cys(42)]	114.3 (5)
S-Fe-S[Cys(39)-Fe-Cys(42)]	112.4 (5)

The initial structural results on *C. pasteurianum* rubredoxin were reported at a slightly lower resolution than those displayed in Table 7.2. In fact, the early study[34] reported a range of Fe-S distances from 2.05 to 2.34 Å. Prior to the higher-resolution refinement, a synchrotron-radiation x-ray-absorption spectroscopy study of the iron-absorption edge of rubredoxin was reported.[35,36] Using the technique of Extended X-ray Absorption Fine Structure,* EXAFS, the average Fe-S distance was found [35,36] to be 2.26 Å, in agreement with the average distance from the x-ray crystallographic study. However, the EXAFS indicated a much narrower permissible range of Fe-S distances than did the early crystallographic study. The later, more highly refined crystallographic treatment[32] agreed nicely with the EXAFS result, illustrating the importance of applying more than one technique to the elucidation of key parameters. Here, as with the 3Fe proteins we will discuss later, EXAFS proved a useful complementary technique to x-ray crystallography.

---

* X-ray absorption spectroscopy is most commonly (and conveniently) used with the K-edges of transition-metal ions, such as Fe or Mo. It can be split up into two distinct types; X-ray Absorption Near-Edge Structure (or XANES), and Extended X-ray Absorption Fine Structure (or EXAFS) spectroscopy. The former consists of features near the absorption edge itself, which are due to transitions of the photoelectron to bound states and also to other, more complex, phenomena (e.g., the so-called shape resonances). Although the spectra are highly dependent on the nature of the site, they are quite difficult to interpret, and most analyses are based upon simple comparisons with spectra from model compounds. The EXAFS are oscillations of the absorption coefficient at rather higher x-ray energies, and arise from scattering of the emitted photoelectron by surrounding atoms. In contrast to the XANES, EXAFS spectra are relatively simple to interpret in a quantitative manner, yielding a local radial structure. With proper interpretation of the spectra, very accurate interatomic distances (e.g., to ± 0.02 Å), plus more approximate ligand coordination numbers and atomic numbers can be obtained.

The tetrahedral iron sites in rubredoxins offer an interesting glimpse of ligand-field theory in action, and illustrate the use of various physical methods in deducing electronic structure and coordination geometry. The four sulfur ligands are expected to split the iron 3d orbitals into e and t_2 sets, with the e set lower as shown in Figure 7.5. The small tetrahedral splitting causes the $3d^5$ Fe^{3+} ion to have five unpaired electrons, $(e)^2(t^2)^3$, $^6A_1$. Consistent with this configuration, the magnetic susceptibility of rubredoxin gives a μ_{eff} of 5.85 Bohr magnetons.[37] No spin-allowed ligand-field transitions are expected, and the red color is caused by S → Fe charge-transfer transitions in the visible region.[38,39]

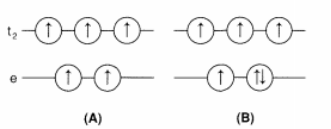

Figure 7.5 - Splitting of the 3d orbitals of Fe by the tetrahedral ligand field of four coordinated cysteine residues: (A) Fe^{3+}; (B) Fe^{2+}.

In contrast, the $3d^6$ Fe^{2+} state, with one additional electron, has four unpaired electrons, as confirmed by its magnetic moment of 5.05 Bohr magnetons. In exact tetrahedral symmetry, a single, low-energy, low-intensity d-d absorption of designation $^5E \rightarrow {}^5T$ $[(e)^3(t_2)^3 \rightarrow (e)^2(t_2)^4]$ is expected for the high-spin ferrous site (Figure 7.5). Indeed, reduced rubredoxin displays a band in the near-infrared region at 6,250 cm^{-1} that arises as a component of the $^5E \rightarrow {}^5T_2$ transition.[40] This band stands out particularly vividly in the low-energy circular dichroism (CD) spectrum of reduced rubredoxin.[41] Moreover, magnetic circular dichroism (MCD) has proven valuable in dissecting electronic transitions in several rubredoxins and metal-sulfide proteins.[38,39,42,43]

The EPR spectrum of oxidized rubredoxin (Figure 7.6) shows characteristic peaks at g = 4.31 and 9.42 (*P. oleovorans*), which have been assigned[44] to transitions within excited and ground-state Kramers doublets, respectively, of a nearly completely rhombic S =

$\frac{5}{2}$ site, with D = 1.8 and E = 0.5 cm^{-1}. These values for the mononuclear Fe^{3+} ion stand in sharp contrast to those for other iron-sulfur proteins, which are usually S = $\frac{1}{2}$ (when reduced) and have g values close to 2. The even-electron Fe^{2+} state (S = 2) in reduced rubredoxin has no detectable EPR when conventional instruments are used.*

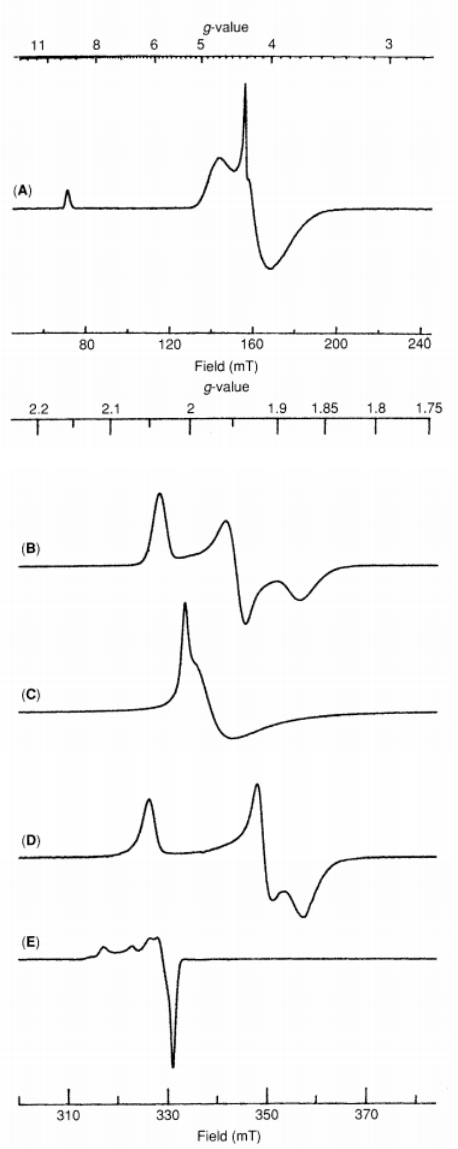

Figure 7.6 - EPR spectra of various Fe-S proteins: (A) oxidized Desulfovibrio gigas rubredoxin; (B) reduced spinach ferredoxin $[Fe_2S_2]^+$; (C) reduced Bacillus stearothermophilus ferredoxin $[Fe_4S_4]^+$; (D) oxidized Thermus aquaticus ferredoxin $[Fe_3S_4]^+$; (E) oxidized Chromatium vinosum HiPIP $[Fe_4S_4]^+$. (Spectra courtesy of S. J. George.)

Mössbauer spectroscopy has proven to be a particularly powerful complementary tool to EPR in probing the iron sites in Fe-S proteins.[3,37,51,52] It is a nuclear spectroscopy that can give valuable information not available from other techniques.† Unlike EPR, where only *paramagnetic* centers are "seen," every ^{57}Fe atom in the sample will contribute to the Mössbauer spectrum. For rubredoxin, the high-spin nature of the ferric and ferrous sites are clearly seen in the Mössbauer spectra.[53] The high-spin Fe^{3+} sites show a small quadrupole splitting of roughly 0.7-0.8 mm/s due to the almost spherical distribution of the five d electrons in the five d orbitals (Figure 7,7A). In contrast, the high-spin Fe^{2+} ion with an additional d electron has a significant asymmetry, and thus displays large and quite characteristic quadrupole splitting of 3.1-3.4 mm/s (Figure 7.7B). The isotope shift also distinguishes between Fe^{2+} and Fe^{3+}, although not as dramatically.[37] Finally, the observation[53] of magnetic hyperfine interaction in the Mössbauer spectrum at low temperature in the Fe^{3+} state directly reveals the presence of unpaired electrons, i.e., magnetic coupling with a hyperfine field of 370 ± 3 kG. Although in rubredoxins with a single Fe atom, this observation of magnetic coupling does not reveal any new information, similar magnetic coupling is particularly useful in unraveling the Fe sites in more complex multiiron proteins.

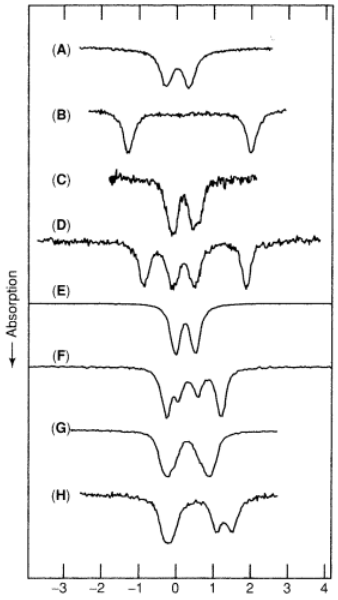

Figure 7.7 - Mössbauer spectra of various Fe-S sites: (A) oxidized and (B) reduced $Fe(SR)_4$ (Fe^{3+} and Fe^{2+}, respectively) rubredoxin models (data from Reference 347); (C) oxidized and (D) reduced Scenedesmus Fe_2S_2 ferredoxin ($2Fe^{3+}$ and [Fe^{3+}, Fe^{2+}], respectively, data from Reference 348); (E) oxidized and (F) reduced Desulfovibrio gigas Fe_3S_4 ferredoxin II ($3Fe^{3+}$ and [$2Fe^{3+}$, Fe^{2+}], respectively, data from Reference 158); (G) oxidized and (H) reduced Bacillus sterothermophilus Fe_4S_4 ferredoxin (data from Reference 349).

* But see Reference 45. EPR spectroscopy uses magnetic fields to split the electron spin states into levels that differ by energy in the microwave region of the spectrum. For an $S = \frac{1}{2}$ system, the g value (and its anisotropy) and the a values (hyperfine splitting from various nuclei and their anisotropy) are the major parameters reported. EPR spectroscopy has played a role in the development of Fe-S biochemistry akin to the role played by optical spectroscopy in the development of the biochemistry of the cytochromes,[46-49] particularly for mitochondria[47] and chloroplasts,[50] where the g = 1.9 EPR signal has facilitated the monitoring of electron flow through these redox systems. Although EPR has been a powerful tool, it does have some important limitations. A necessary but not sufficient condition for EPR is that the center to be observed must be in a paramagnetic state. Fortunately, this condition is met for at least one member of each one-electron redox couple, i.e., the odd-electron species. However. even when the even-electron species is paramagnetic, it is usually not observed in the EPR, because of the presence of large zero-field splittings. Moreover, relaxation effects and/or the population of excited states often cause the EPR of proteins to be unobservable at room temperature. necessitating the use of liquid N_2 or liquid He temperatures to observe the signals in the frozen state. The need to freeze samples prior to observation can lead to artifacts involving the observation of nonphysiological states and processes. On the positive side, the low temperature increases the signal intensity by altering the Boltzmann distribution of the spin population, and allows various quenching techniques to be used with EPR to evaluate kinetic and electrochemical parameters. Nevertheless, one cannot usually observe real-time kinetics or be certain that one is observing a physiologically relevant state. Despite these caveats, EPR has proven a valuable and, in some cases, indispensable tool for identification and monitoring of Fe-S sites. Recently, the advanced EPR techniques ENDOR (Electron Nuclear Double Resonance) and ESEEM (Electron Spin Echo Envelope Modulation) have allowed the extraction of additional information from the EPR signal.

† Mossbauer spectroscopy measures nuclear absorption of light at γ-ray energies, and can be used to probe nuclear energy levels (usually of ^{57}Fe). The splitting of these levels is influenced by the (s) electron density at the nucleus, and by the electric-field gradient that is set up by nearby atoms. These factors affect the isomer shift and the quadrupole splitting of the Mössbauer spectrum, respectively. Information on nuclear hyperfine couplings is also available when experiments are conducted in the presence of an external (usually applied) magnetic field. Fortunately, the nucleus most commonly (and easily) studied by this technique is present in all the proteins discussed in this chapter, although the level of ^{57}Fe (2 percent natural abundance) must be increased by isotopic enrichment to achieve a high-enough signal-to-noise ratio. For spectra containing one type of site, the spectra are relatively straightforward to interpret. For multisite systems deconvolution is required to get data on individual centers. When possible, selective labeling of sites with ^{57}Fe is extremely helpful in the deconvolution process.

NMR studies on both the oxidized and the reduced states of rubredoxins have been reported. The strongly paramagnetic iron atoms have a profound effect on the NMR spectra of protons in the vicinity of the iron. The iron drastically affects the relaxation behavior of such protons, causing line-broadening, sometimes so much that the protons become nonobservable. If observed, the protons are shifted far from the values found in diamagnetic proteins by combinations of Fermi contact (through overlap/through bond) and pseudo-contact (through space/dipolar) coupling.[54,55] In the rubredoxins, the reduced state shows resolved spectra,[37,56] which can be assigned[56] with the help of data from model systems.*

Resonance Raman spectroscopy provides information involving molecular vibrations that is not dependent on either nuclear or magnetic properties. Electronic excitation of bands involving S → Fe charge transfer often leads to resonance enhancement of Fe-S stretching modes. In rubredoxin,[57,57a] the Fe-S stretching vibrations are located between 300-400 cm^{-1}. Deviations of the expected two-band tetrahedral pattern (T_2 and A_1 modes) are attributable to coupling of the Fe-S vibrations with S-C-C bending modes. This coupling makes for greater variability, and the detailed vibrational assignment is thus more difficult for bands involving the cysteinyl sulfur atoms. In contrast, for sites containing inorganic S^{2-}, the Fe-S vibrations involving the inorganic core are less variable and therefore more characteristic of the core type.[57]

In theory, each of the spectroscopic techniques applied to rubredoxins can give useful information about the other iron-sulfur proteins. In practice, some techniques have proven more useful than others in particular situations, and combined use of several techniques is necessary to draw meaningful conclusions.

Chemical studies of rubredoxins have led to the replacement of the Fe^{2+} with an Fe_4S_4 center,[58] with Co^{2+}, and with Ni^{2+}. The Co^{2+} replacement of Fe^{2+}, in *P. oleovorans* rubredoxin, leads to a stable protein that displays reduced (but not trivial) reactivity in the ω-hydroxylation reaction.[59,60] The spectral properties of the cobalt(II) site show the expected changes in d-d bands and the expected shifts in charge-transfer transitions.[59] Interestingly, when Ni^{2+} is substituted into rubredoxins from desulfovibrio species, the resultant proteins show hydrogenase activity.[61]

---

* NMR is a technique whose great utility in the study of low-molecular-weight proteins and model systems has not (yet) carried over to the study of larger proteins. Slower tumbling rates, rapid electronic relaxation, multiple paramagnetic sites, large numbers of protons, and more dilute solutions conspire to make the observation and/or interpretation of NMR spectra a daunting task in multisite redox proteins of > 50 kDa.
